

# End-Effector Pose Estimation and Control for 3D Printing with Articulated Excavators

**Conference Paper****Author(s):**

Malczyk, Grzegorz ; Hutter, Marco 

**Publication date:**

2023

**Permanent link:**

<https://doi.org/10.3929/ethz-b-000635978>

**Rights / license:**

In Copyright - Non-Commercial Use Permitted

**Originally published in:**

<https://doi.org/10.1109/ICAR58858.2023.10406417>

# End-Effector Pose Estimation and Control for 3D Printing with Articulated Excavators

Grzegorz Malczyk, Marco Hutter

**Abstract**—We introduce a novel large-scale autonomous mobile manipulator system based on an instrumented and automated construction machine for precise on-site sensing and fabrication. The system is based on an automated hydraulic walking excavator equipped with IMUs and LiDAR units. In this work, we develop the technology to precisely map, localize, and move the printhead in the environment. By fusing GNSS localization with kinematic sensing of the mobile machine and end-effector, we get a globally consistent and locally accurate positioning for in situ robotic construction printing process. Moreover, we present a control approach that enables the excavator to move the end-effector precisely along predefined trajectories. We evaluate the performance of the proposed system in a variety of real-world tests in the field and analyze different sensor modalities and arrangements. Finally, we discuss the potential applications, including the fabrication of non-standard architectural forms and increased safety.

**Index Terms**—pose estimation, precise control, 3D printing, large-scale fabrication

## I. INTRODUCTION

Construction shapes our modern world, and the application of onsite 3D printing in construction has become a very relevant construction technique. Primarily, it requires the broad printhead reach of the 3D fabrication robotic process and high local accuracy in positioning. However, so far, 3D manufacturing, like concrete printing requires large infrastructure installations such as a gantry setup to move the printhead precisely along predefined trajectories [1]. Due to the size and complexity of the necessary gantry installation, such fabrication processes are predominantly found in pre-fabrication and rarely find their way into onsite or in-situ construction [2]. Setting up the gantry-type printing infrastructure on hillsides or in remote locations becomes even less feasible and asks for new solutions. It makes such systems relatively expensive to set up because of a temporary installation of a manufacturing and assembly hall and allows their use only in case of sufficient space and good accessibility [3]. To overcome the limitations of current printing processes, we want to build upon existing and commonly used mobile construction machines paired with novel control technologies for automation and high-precision printhead positioning. Such a setup effectively extends the scale of printable structures and even opens the potential to deploy such systems in locations where expensive construction installations are unavailable.

### A. Related Work

1) *Printing onsite machines*: Digital fabrication technologies, including robotic fabrication and 3D printing, promise to empower the development of customized material systems



Fig. 1. The autonomous walking excavator HEAP equipped with an assembly gripper [4].

and building components within the domain of architecture and construction, enabling entirely new approaches to the design of architectural structures [5], [6]. One of the concepts with a quasi-stationary man-lift and Kuka robot arm as the end-effector was used in the work by Keating [7]. Due to the higher complexity of machine positioning, only a few solutions leverage the advantage of mobile systems in construction, and most of them still use classical industrial robot arms with limited payload, heavyweight, and low robustness. As such, these systems typically also work in a quasi-static and kinematically controlled manner, whereby the system base is localized, and the arm is controlled in a purely kinematic fashion. Those solutions have been realized in modern research prototypes [8] or in commercial products [9], but they all rely on very stiff kinematic arm control. Unfortunately, such an approach does not work in construction machines: imprecise kinematics, moving base, play and compliance in joints make it almost impossible to apply pure kinematic position control. To overcome these limitations, it is crucial to localize the end-effector relative to the building structure [10], [11] as done in classical visual servoing applications. In this paper, we propose an innovative approach to onsite additive manufacturing, which consists of an automated, highly mobile construction machine HEAP equipped with a precisely controllable material printing device (Fig. 1), as such it can overcome the limitations of fixed installations while offering almost unlimited reach.

2) *Perception and end-effector localization*: Most construction machines on the market cannot track their poses relative to some project coordinate frames of interest. There are several methods employed so far to control and estimate the pose of an articulated machine, especially the system end-

effector.

First are the 2D or stereo video-based methods, inspired by the progress in computer vision on object recognition and tracking. Static surveillance cameras were used to track the motion of a tower crane in [12] for activity understanding. This method generally requires no retrofitting on the machine but suffers from both possibilities of false or missed detection due to the complex visual appearance on job sites and the relatively slow processing speed. Although real-time methods exist as in [13], [14], they either cannot provide accurate 6D pose estimation, or require additional information such as a detailed 3D model of the machine. In [15], the shovel's swing rotation was recovered using stereo vision SLAM, yet the pose of its bucket was not estimated. This approach can be infrastructure-independent, yet some problems, like the sensitivity to lighting changes or texture-less regions of the printed structures, remain to be resolved for more robust robotic applications.

Next, instead of measuring all points in the visible environment, an external measurement system, such as a robotic total station, can be employed to measure the distance to a reference point, e.g. a reflector prism. Several approaches have been suggested involving the use of a total station for the localization of mobile robots in construction. One such approach involves placing the measurement device on the mobile robot base [16], [17] or on the robot end-effector [18], and the total station carries out sequential measurements within an environment. Although the method ensures a high-accuracy estimate of the end-effector position in the unstructured world environment, it comes with minor limitations. Primary, requiring a clear line of sight from the reflector prism to the measurement device. Moreover, such a system lacks the perception component, which is essential for robotic fabrication in the context of construction sites, but only targets a precise pose estimation from point-to-point measurements. Additionally, this approach is often employed for small robotic arms and not with large-scale construction machines, like excavators.

Finally, the laser-based methods [19]–[21]. These pipelines can yield good pose estimation accuracy if highly accurate dense 3D point clouds of the scene are observed using expensive and heavy laser scanners and remove the need for fixed reference points for the localization. Otherwise, with low-quality 2D scanners, only decimeter-level accuracy was achieved [20].

### B. Contribution

In this work, we investigate a LiDAR-based solution for end-effector pose estimation with heavy articulated machines. The proposed setup scans the construction environment and localizes the printhead with a sub-centimetre accuracy of 5.8 mm in the generated map during the printing process. We compare our method against a well-established kinematic sensing approach for end-effector localization in real-world experiments on the large-scale excavator. Furthermore, we benchmark both methods against the ground truth obtained with the robotic total station to examine various sensor

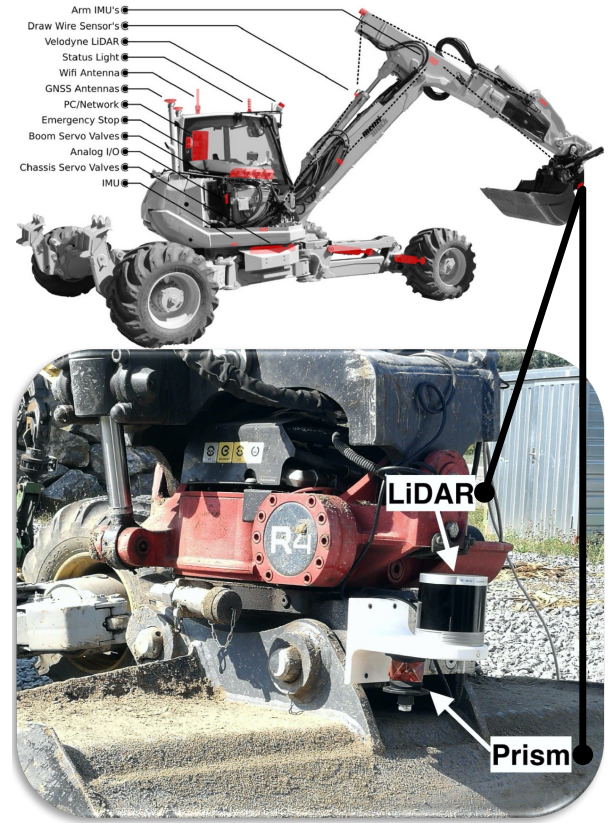


Fig. 2. Sensor and actuation setup of the customized Menzi Muck M545 [4]. Below, the experimental sensors module consists of the LiDAR and the reflector prism mounted at the tip of the excavator's arm.

arrangements. Lastly, we employ the LiDAR-based pose estimation in the end-effector tracking control problem and report a maximum global error of 4.4 cm.

## II. HARDWARE SETUP

HEAP is a platform based on a commercially available 12t Menzi Muck M545 walking excavator with a 4300 kg lift capacity in the fully stretched arm position. The machine has been highly customized with numerous adaptations and additions (see Fig. 2). A Leica iCON with two GNSS antennas is used for cabin localization. RTK corrections for the GNSS signals are received over the internet from permanently installed base stations. The IMUs, in both the cabin and the chassis, complement these position sensors and allow for a full 6 degrees of freedom (DOF) pose estimation of the cabin. The arm joint states are measured concurrently by drawing wire encoders on the hydraulic cylinders and IMUs on the links. A detailed description of the employed sensor setup, chassis and arm actuation strategies can be found in [4].

In order to evaluate different methods for end-effector localization in the construction environment, we designed a mount which we attach at the manipulator tip, see Fig. 2. A LiDAR and the reflector prism are used for localization and ground truth measurement validation respectively. The LiDAR is chosen because it outperforms camera-based sensors in heavy dust environments and provides more accurate and dense measurements compared to radar-based sensors [22].

### III. METHODS

For localization of the end-effector, the straightforward way is to use the existing localization of the base from GNSS paired with kinematic sensing of the arm to get the relative offset of the end-effector wrt base. We describe this baseline method in the first part. Since onsite 3D printing requires high accuracy to accomplish the desired architectural design plan, we investigate various setups to provide highly accurate localization of the end-effector in an unstructured outdoor environment. Thus, to further enhance end-effector pose estimate precision, one includes additional measurements of the position of the end-effector wrt to the world using either a total station prism or LiDAR mounted at the manipulator tip. We present this improved method in the second part of this section. Thereby, we highlight their advantages and drawbacks and demonstrate how we can achieve sub-cm precision with large-scale construction machines.

#### A. Kinematic sensing

To estimate the 6-DOF end-effector pose, we fuse IMUs measurements of the cabin with GNSS sensing to get a precise base pose estimation and combine this with a relative end-effector to base pose using joint sensors (cabin and telescopic joint) and link IMUs mounted on the arm [4]. The estimated state contains the position and the orientation of the end-effector. The error in the GNSS signal can vary in the range between 1 up to 10 cm, and the forward kinematics of the arm joints become significant if the load is applied at the tip of the articulated arm. We use the pose estimator from [4] as a baseline and compare our approach against it.

*Cabin turn joint:* The position measurement of the cabin turn joint connecting the upper machine to the chassis is realized with two inductive sensors that detect passing gear teeth. An additional inductive sensor corrects potential errors of this incremental measurement when passing zero. Due to the low number of teeth in the large internal ring gear (98 teeth in total), an angular resolution of only 0.92 deg can be achieved. Due to these measurements' low resolution, we estimate the absolute pose of the cabin from IMU and GNSS and relative turn using a Kalman filter (KF). Thus, the joint state (position  $\psi$  and velocity  $\psi'$ ) is estimated in the cabin frame, where the sensors are rigidly attached. The cabin turn angular velocity is measured as the difference between the angular velocities of the cabin IMU and the chassis IMU. The state of the cabin joint is obtained using the discrete-time KF to augment the noisy IMU angular velocity and low-quality turn angle measurements. The position and velocity of the joint are described by the linear state space:

$$\mathbf{x}_k = [\psi, \psi']^T \quad (1)$$

Under the assumption that velocity between the  $(k-1)$  and  $k$  timestep is constant, we conclude the prediction model

$$\mathbf{x}_k = \begin{bmatrix} 1 & \Delta t \\ 0 & 1 \end{bmatrix} \mathbf{x}_{k-1} + \mathbf{w}_k \quad (2)$$

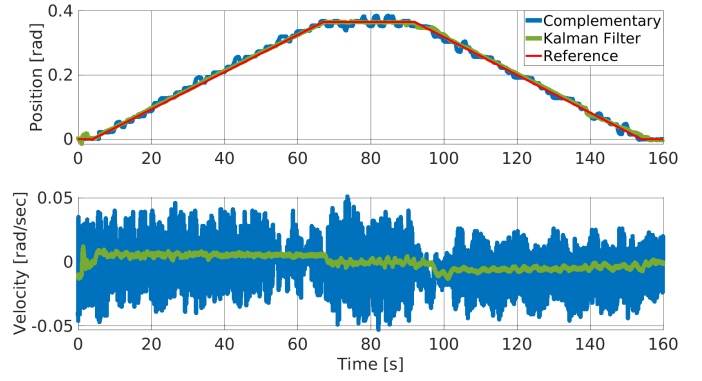


Fig. 3. In blue, the complementary filter while the KF estimate in green. In red, we indicate the reference joint position.

where  $\mathbf{w}_k \in \mathbb{R}^2$  represents the process state noise. At each time phase, noisy measurements of the joint position and velocity are made. Thus, the observation model reads

$$\mathbf{z}_k = \begin{bmatrix} 1 & 0 \\ 0 & 1 \end{bmatrix} \mathbf{x}_k + \mathbf{v}_k \quad (3)$$

where  $\mathbf{v}_k \in \mathbb{R}^2$  is the measurement noise.

Compared to [4], where one implements a complementary filter for the cabin turn joint, we account for a low-resolution joint position measurement and sensor noise while ensuring a smooth estimate signal, as presented in Fig.3. The complementary uses raw angular velocity data and computes the turn angle estimate with the weighting factor for joint position measurement. In the two consecutive experiments in Fig.3, we command the same reference position for the joint while once running the complementary filter and once using the KF method. The average tracking error of the position is 0.002 rad with the KF approach while 0.028 rad with complementary filter. The Kalman filter approach considers sensor noise and captures different update rates of incoming measurements while enabling the precise rotational motion of the cabin at the very-low velocities. This is becoming crucial while we aim to improve the end-effector positioning for the highly accurate following of the printhead trajectories.

#### B. Total station

Following [18], the localization of the mobile printer in reference to the total station is investigated through the positioning of a reflector prism attached to the robot's end-effector. The total station measures the prism position in an environment in the frame defined by the human operator. The total station used in the project is a Leica Nova MS50 MultiStation and a reflector prism Mini GRZ101 360°. The MS50 offers an angular accuracy of 1'' and an optical-distance measurement system (EDM) based on waveform digitizing technology with an accuracy of 1 mm onto the prism and a measurement range of around 1000 m. The prism mount provides flexibility in setting trajectories within the robot workspace as reference points and a clear line of sight between the end-effector and the total station. The calibration between the robot and global (total station) frames considers arbitrary point selection. For the point set registration problem, multiple



algorithms exist [23]. By moving the excavator arm in the workspace to  $n$  various locations, the prism coordinates of  $n$  points  $P_i \in \mathbb{R}^{6 \times 1}$  in the robot coordinate frame, and the  $n$  prism measurements  $M_i \in \mathbb{R}^{3 \times 1}$  in the total station coordinate frame are derived. Through orthogonal decomposition of the points  $P_i$  in the total station coordinate frame and corresponding measurements  $M_i$ , we compute a transformation matrix  $\mathbf{T}_{M,P}$ , which maps the measurements into a robot reference frame.

$$\mathbf{T}_{M,P} = [P_1 \ P_2 \ \dots \ P_n] \times [M_1 \ M_2 \ \dots \ M_n]^\dagger \quad (4)$$

where  $n > 4$  to obtain a unique solution.

The computed transformation matrix enables control of the mobile 3D printer end-effector based on the total station readings. Although the method ensures a high-accuracy estimate of the end-effector position in the construction environment, it comes with minor limitations. Primary, this approach requires a direct line of sight from the reflector prism on the end-effector to the total station at any time during fabrication. As a result, avoiding the prism occlusion strongly limits the printer workspace.

### C. ICP Localization

To target the accuracy of global positioning with an onboard-sensing system only, we employ a LiDAR at the end-effector. This device is primarily used for running pure ICP (Iterative Closest Point) with the environment and provides an ultra-wide view. First, we scan the construction site with the sensor attached to the tip of the articulated arm assuming static features in the environment. In offline manner, we build a map that serves as the reference for online localization of the 3D printer during construction tasks. For this, we make use of the open-sourced package *open3d\_slam* [24], and obtain the map of the construction site, as depicted in Fig. 4. The package is implemented based on Open3D, a library for 3D data processing. This method eliminates the requirement of a clear line of sight, as different stationary features of the environment are observed at any time. During deployment, these specific features in the map are utilized to localize the printhead in the global frame through scan matching using ICP scan-to-map registration. We fine-tune the hyper-parameters of the ICP algorithm to get high precision in the pose estimation and achieve an error in accuracy below 1 cm.

### D. Multi measurement fusion

The rate of the pose estimate based on the ICP pipeline is constrained by the low-frequency update measurement of the LiDAR (10 Hz). To increase the smoothness of the estimated signal and allow for fast and precise end-effector motions, we fuse the ICP updates with kinematic measurements collected at high frequency (100 Hz). This sensor fusion is based on an extended Kalman filter (EKF) to track the orientation and position of the end-effector. The fusion framework is essentially divided into two EKF steps: prediction and update. The prediction step is preformed based on the system model (assuming constant velocity) and kinematics readings [25]. In situations between subsequent LiDAR measurements, we

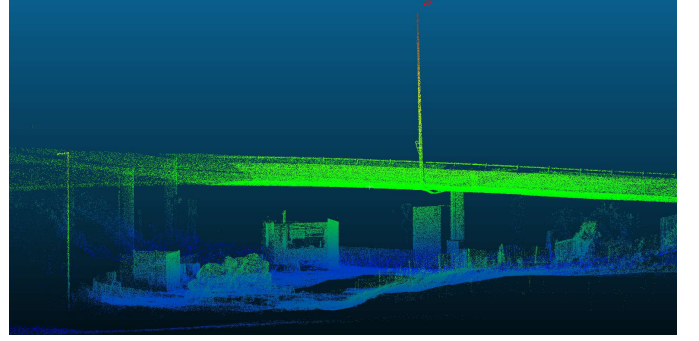


Fig. 4. The map is built on the construction site with the *open3d\_slam* library. The barracks are on the left, and the bridge with columns is on the right.

interpolate the kinematics data to get the best possible end-effector pose estimate. These kinematic measurements are coming from IMUs mounted across the excavator's arm and joint position encoders (cabin and telescopic joint), as described in Sec. III-A. For the EKF update step, we incorporate data obtained with the ICP localization pipeline. Thus, by fusing kinematics and LiDAR measurements, the printhead positioning precision is improved, and the final end-effector pose estimate remains consistent in the global reference frame while being updated on 100 Hz.

## IV. EXPERIMENTAL RESULTS

Before implementing the pose estimation system pipeline, we perform a set of experiments to test the feasibility of LiDAR-based pose estimation in different indoor and outdoor construction environments. In all the experiments, a Hesai QT64 LiDAR is chosen with a 20 m range and vertical resolution of 104.2 deg. Instead of using the entire map for localization, we restrict it to selected objects that remain stationary throughout the fabrication process and provide clear features for localization, such as bridge and barrack, see Fig. 4.

Next, the accuracy of the ICP localization is a critical factor affecting the performance of the fabrication process. Thus, the LiDAR is tested in the indoor (office room  $\approx 30 \text{ m}^2$ ) and outdoor conditions to examine its robustness and repeatability. After building the map of the environment, we start the localization method while subsequently recording the sensor pose obtained with the *open3d\_slam* library at different times. In Tab I, we report an average error between the ICP localization measurements obtained from the set of recorded poses in indoor and outdoor experiments. In the outdoor scenario, we encounter different light circumstances as the runs are performed at different times of the day facing various environmental conditions. On the other hand, to ensure the precise localization required by the 3D printing process, we examine the scenarios assuming that clear reference points exist. This initial analysis validates the deployment of the LiDAR-based localization method to obtain high-accuracy and repeatable performance in pose estimation. As the sensor remains stationary during this experiment, the error mostly comes from the device noise. The deviation is higher outdoors as the LiDAR experiences more demanding lighting

TABLE I  
ERROR IN THE ICP POSE ESTIMATE

		indoor	outdoor
Position error [cm]	x	0.12	0.35
	y	0.08	0.47
	z	0.02	0.19
Orientation error [deg]	roll	0.12	0.34
	pitch	0.23	0.61
	yaw	0.19	0.45

conditions and a larger distance to the environmental features. Nonetheless, the error lies below the precision requirements for the 3D printing process, i.e. below 1 cm [26]. Once the sensor achieves the distance of 20 m from the reference features, we obtain an error above the sub-centimetre level accuracy. Thus, we require the environmental references to lie within this radius from the end-effector. From now on, all the experiments are performed with the real construction machine [4].

#### A. End-effector localization

In this experiment, we manually steer the excavator arm from inside the cabin with an arbitrary end-effector trajectory, shown in Fig. 5. During this experiment, we analyze the state estimation methods introduced above, namely the baseline (kinematic sensing) method and ICP localization. We compare them against the total station readings, as these measurements provide the ground truth end-effector pose. We present the performance of both state estimation methods in Fig. 6 against the ground truth, both expressed in the world frame.

The root mean square error (RMSE) with the LiDAR localization approach is 0.58 cm, while with the baseline method, we report 2.23 cm. The error lies in the interval within  $\pm 1$  cm from the ground truth over 96% of time for the ICP method and 49% in the case of the kinematic sensing approach. The maximal positioning error for ICP is 1.87 cm while 6.61 mm with the baseline. The experiment outlines the advantage of using the LiDAR-based pose estimation for the excavator end-effector during the fabrication processes when the highly accurate localization is a crucial factor while following the predefined architectural plan.

#### B. Experimental 3D printing end-effector path

Each end-effector task is described as a predefined trajectory composed of a time series of printhead poses according to the architectural design plan. The task should be executed as a continuous motion, while the 3D printer should smoothly pass through each waypoint. We use cubic Hermite trajectory interpolation<sup>1</sup> to obtain smooth paths for the system between the subsequent design poses. Then the polynomial trajectory is sampled at 100 Hz and passed to the controller as an array of reference points.

<sup>1</sup><https://github.com/ethz-asl/curves>

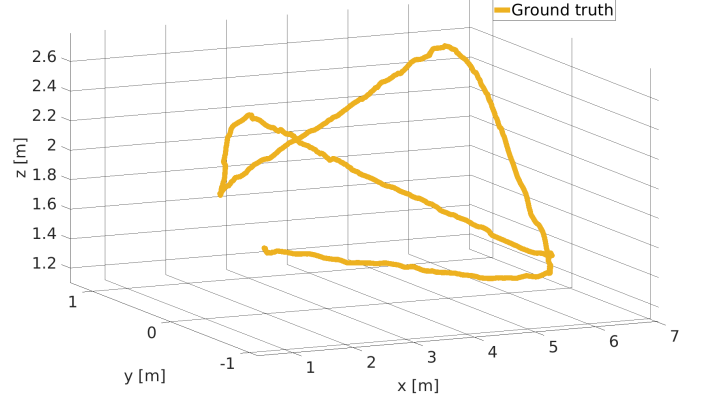


Fig. 5. The ground-truth trajectory of the excavator's arm end-effector depicted in the world frame obtained with the total station.

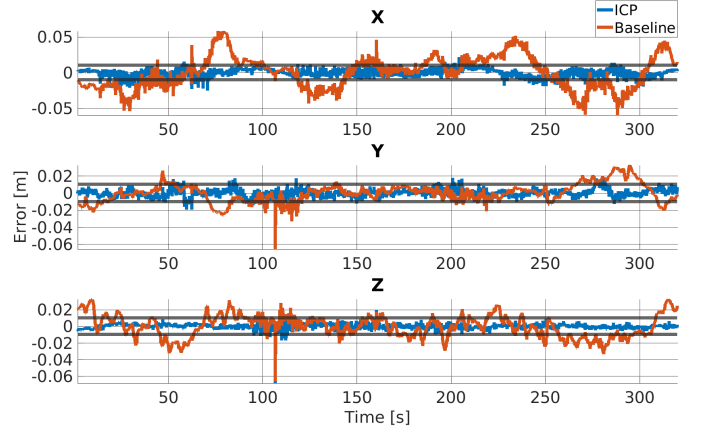


Fig. 6. Error plot between the two end-effector state estimators and total station measurements. In orange, we depict the error recorded with the baseline approach and in blue with the ICP localization pipeline, along  $x$ ,  $y$  and  $z$  in the world frame, respectively. Additionally, we indicate the 1 cm error range from the ground-truth measurement in grey horizontal lines.

#### C. End-effector tracking performance

As a last experiment, we close the control loop with the LiDAR-based localization approach. We provide the arm controller with the end-effector pose estimate obtained from the ICP pipeline. This showcases how accurately the machine can track the desired trajectories during the 3D printing process while the printhead pose estimation has been improved. The trajectory, shown in Fig. 7, is defined in the map frame. We report the tracking error performance during this process. The maximum deviation from the reference path is 3.8 cm, and the overall RMSE is equal to 0.9 cm.

With results from Sec. IV-A, we conclude that the average global error during fabrication is 1.5 cm, which outperforms the 3D printing with flying robots (precision of 10 cm) and is comparable with mobile industrial robotic arms equipped with a high-precision 3D motion capture system (average error of 1.0 cm) [26].

## V. CONCLUSION

Excavator systems are ubiquitous on construction sites. Equipped with the right sensing and control technology, they offer the potential to serve as precise tool manipulators that

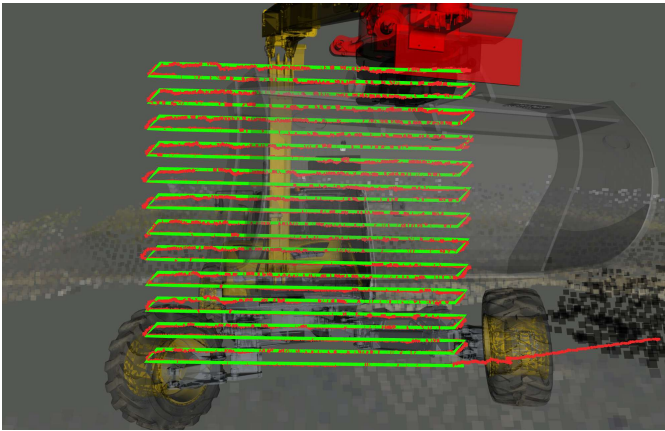


Fig. 7. End-effector 3D printing desired trajectory is depicted in green, while in red, we show the measured printhead pose obtained with the ICP.

can be used for tasks like onsite 3D printing. In this paper, we investigated different sensor arrangements and localization solutions. Using IMUs at the moving links, GNSS at the cabin and a LiDAR at the end-effectors, we are able to achieve 5.8 mm localization precision at the end-effector. This paper focuses on a LiDAR-based pose estimation and localization solution for articulated machines using ICP in a known map. A sensor system consisting of LiDAR and kinematic sensing across the articulated arm of the large-scale machine offers a potential alternative to the solution with the total station and eliminates the problem of a clear line of sight for the prism. Moreover, the approach does not require an external measurement system as the mobile industrial robotic arms, which are equipped with a 3D motion capture system for 3D printing. We validate the method with an error analysis to assess the system position accuracy. The presented experiments and a working prototype proved the proposed solution's feasibility and accuracy for real-world construction applications. In addition, various fabrication methods using a range of end-effectors, such as a 3D printer, an assembly gripper, or a welding tool, can be implemented as part of the fabrication process. Through these capabilities the system is designed to complete the large-scale toolchain, providing real-time digital sensing, on-the-fly performance-based design, and onsite construction. By combining sensor data with material deposition logic the designer will be able to respond to site-specific terrain mapping in real time.

In future work, we investigate the feasibility of the measurement system while making full use of the excavator manipulator structural characteristics, i.e. by employing the motion of the excavator chassis. Additionally, we aim to demonstrate the use of large-scale mobile manipulators utilizing 3D printers for the construction of complex architectural forms.

## REFERENCES

- [1] B. Khoshnevis, "Automated construction by contour crafting—related robotics and information technologies," *Automation in construction*, vol. 13, no. 1, pp. 5–19, 2004.
- [2] L. Nanz, M. Rauch, T. Honermann, and T. Auer, "Impacts on the embodied energy of rammed earth façades during production and construction stages," *Journal of Facade Design and Engineering*, vol. 7, no. 1, pp. 75–88, 2019.
- [3] S. Huang, W. Xu, and Y. Li, "The impacts of fabrication systems on 3d concrete printing building forms," *Frontiers of Architectural research*, vol. 11, no. 4, pp. 653–669, 2022.
- [4] D. Jud, S. Kersch, M. Wermelinger, E. Jelavic, P. Egli, P. Leemann, G. Hottiger, and M. Hutter, "Heap-the autonomous walking excavator," *Automation in Construction*, vol. 129, p. 103783, 2021.
- [5] M. Bechthold, "The return of the future: a second go at robotic construction," *Architectural Design*, vol. 80, no. 4, pp. 116–121, 2010.
- [6] R. Glynn and B. Sheil, *Fabricate 2011: Making Digital Architecture*. UCL press, 2017, vol. 1.
- [7] S. J. Keating, J. C. Leland, L. Cai, and N. Oxman, "Toward site-specific and self-sufficient robotic fabrication on architectural scales," *Science robotics*, vol. 2, no. 5, p. eaam8986, 2017.
- [8] M. Gifthalder, T. Sandy, K. Dörfler, I. Brooks, M. Buckingham, G. Rey, M. Kohler, F. Gramazio, and J. Buchli, "Mobile robotic fabrication at 1: 1 scale: the in situ fabricator: system, experiences and current developments," *Construction Robotics*, vol. 1, pp. 3–14, 2017.
- [9] O. H. Rosenlund, "Mobile drilling robot-a case study of the effects on the construction site," Master's thesis, NTNU, 2017.
- [10] M. Lussi, T. Sandy, K. Dörfler, N. Hack, F. Gramazio, M. Kohler, and J. Buchli, "Accurate and adaptive in situ fabrication of an undulated wall using an on-board visual sensing system," in *IEEE International Conference on Robotics and Automation (ICRA)*, 2018, pp. 3532–3539.
- [11] T. Sandy, M. Gifthalder, K. Dörfler, M. Kohler, and J. Buchli, "Autonomous repositioning and localization of an in situ fabricator," in *IEEE International Conference on Robotics and Automation (ICRA)*, 2016, pp. 2852–2858.
- [12] J. Yang, P. Vela, J. Teizer, and Z. Shi, "Vision-based tower crane tracking for understanding construction activity," *Journal of Computing in Civil Engineering*, vol. 28, no. 1, pp. 103–112, 2014.
- [13] M. Memarzadeh, A. Heydarian, M. Golparvar-Fard, and J. Niebles, "Real-time and automated recognition and 2d tracking of construction workers and equipment from site video streams," in *Computing in Civil Engineering (2012)*, 2012, pp. 429–436.
- [14] J. D. Brookshire, "Articulated pose estimation via over-parametrization and noise projection," Ph.D. dissertation, MIT, 2014.
- [15] L.-H. Lin, P. D. Lawrence, and R. Hall, "Robust outdoor stereo vision slam for heavy machine rotation sensing," *Machine vision and applications*, vol. 24, pp. 205–226, 2013.
- [16] D. Bouvet, G. Garcia, B. J. Gorham, and D. Bétaille, "Precise 3-d localization by automatic laser theodolite and odometer for civil-engineering machines," in *IEEE ICRA*, 2001, pp. 2045–2050.
- [17] H. Halvorsen, T. A. Henning, and K. Fagerun, "Mobile robotic drilling apparatus and method for drilling ceilings and walls," Nov. 15 2018, uS Patent App. 15/522,951.
- [18] S. Ercan, S. Meier, F. Gramazio, and M. Kohler, "Automated localization of a mobile construction robot with an external measurement device," in *36th International Symposium on Automation and Robotics in Construction (ISARC)*, 2019, pp. 929–936.
- [19] E. Duff, "Tracking a vehicle from a rotating platform with a scanning range laser," in *Australian Conference on Robotics and Automation*, 2006.
- [20] A. H. Kashani, W. S. Owen, N. Himmelman, P. D. Lawrence, and R. A. Hall, "Laser scanner-based end-effector tracking and joint variable extraction for heavy machinery," *The International Journal of Robotics Research*, vol. 29, no. 10, pp. 1338–1352, 2010.
- [21] Y. K. Cho and M. Gai, "Projection-recognition-projection method for automatic object recognition and registration for dynamic heavy equipment operations," *Journal of Computing in Civil Engineering*, vol. 28, no. 5, p. A4014002, 2014.
- [22] T. G. Phillips, N. Guenther, and P. R. McAree, "When the dust settles: The four behaviors of lidar in the presence of fine airborne particulates," *Journal of field robotics*, vol. 34, no. 5, pp. 985–1009, 2017.
- [23] F. Pomerleau, F. Colas, R. Siegwart *et al.*, "A review of point cloud registration algorithms for mobile robotics," *Foundations and Trends® in Robotics*, vol. 4, no. 1, pp. 1–104, 2015.
- [24] E. Jelavic, J. Nubert, and M. Hutter, "Open3d slam: Point cloud based mapping and localization for education," in *ICRA Workshop on Robotic Perception and Mapping: Emerging Techniques*, 2022.
- [25] S. Lynen, M. Achtelik, S. Weiss, M. Chli, and R. Siegwart, "A robust and modular multi-sensor fusion approach applied to mav navigation," in *IEEE/RSJ IROS*, 2013, pp. 3923–3929.
- [26] Z. Xu, T. Song, S. Guo, J. Peng, L. Zeng, and M. Zhu, "Robotics technologies aided for 3d printing in construction: A review," *The International Journal of Advanced Manufacturing Technology*, vol. 118, no. 11–12, pp. 3559–3574, 2022.